Advanced Radiance Transformation System (ARTS) For Space-borne Microwave Instruments

Hu(Tiger) Yang[1], Fuzhong Weng[2], Ninghai Sun[2]
Wanchun Chen[2], Lin Lin[2] , Miao Tian[1]

1. Earth Science System Interdisciplinary Center, University of Maryland
2. NOAA Center for Satellite Applications and Research, USA
huyang@umd.edu

Nov 12, 2014

Introduction

NOAA request a full radiance based calibration algorithm for consistent calibration for historical, present and future microwave sounding instruments

- Weather forecast application require continuous improving for satellite instrument calibration accuracy
- Satellite climate study need to develop and implement a robust, sustainable and scientifically defensible calibration system to producing and preserving climate records from satellite data

Present microwave calibration system is derived in temperature space, which is not consistent with historical full radiance calibration system developed in NOAA

- R-J approximation corrected calibration algorithm will cause scene dependent calibration error
- New sciences established from solid study of SNPP ATMS are need to be included to improve the calibration accuracy

An Advanced Radiance Transformation System (ARTS) is developed for microwave sounding instruments in JPSS era

- Full radiance calibration system applicable to different sensors
- New science for improving the calibration accuracy

ARTS System and Software Engineering

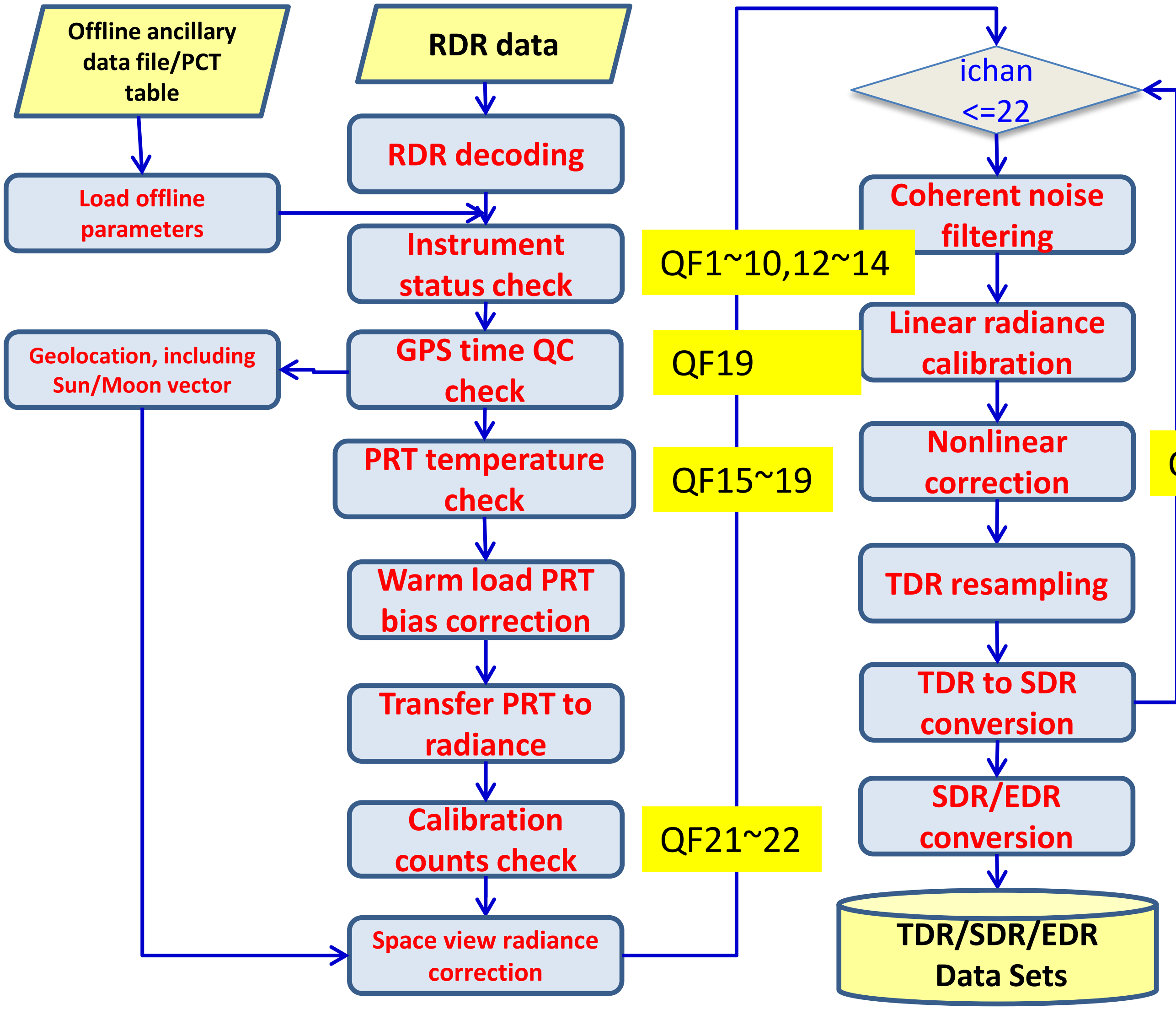

- Consistent calibration algorithm for different sensors
- Full radiance calibration system with improved two-point calibration algorithm
- Data resampling ability to generate TDR with different spatial resolutions

Quality Control in ARTS

Different level of Quality control with PCT as inputs makes system being sustainable

Granule Level

- QF11: Nonlinearity Correction

Scan Level

- QF1~10: Status of Health items
- QF12~14: Warmload/Shelf PRT Conversion quality
- QF15~18: Out of range and consistency check for PRT temperature
- QF19: Scan time/Data gap/PRT sufficiency check; Scan position error check

Channel Level

- QF20: Moon in space view check; Gain error check; insufficient calibration counts check;
- QF21: Space view/Warmload view out of range check
- QF22: Space view/Warmload view inconsistency check

Supported Platforms

- Supports both big and little endian platforms
- Comparable processing efficiency with IDPS

OS	C compiler	C++ compiler	Fortran 90 compiler
AIX 5.3.0.0 or later	IBM XL C/C++ Enterprise Edition for AIX, V10.1	IBM XL C/C++ Enterprise Edition for AIX, V10.1	IBM XL Fortran Enterprise Edition for AIX, V12.1
LINUX (Red Hat Enterprise 5)	GCC 4.3.2	GCC 4.3.2	Intel Fortran version 11 or later
Windows XP/Vista running Cygwin	GCC 4.3.2	GCC 4.3.2	gfortran

Main ARTS Modules

- Satellite geolocation/validation
- Full radiance calibration/validation
- Nonlinearity correction
- B-G remapping
- Coherent noise filtering
- Lunar contamination correction

Geolocation

- Geolocation module includes GPS based and TLE based algorithms
- Primary algorithm uses GPS measurements of satellite position/velocity
- TLE is used as backup when no GPS data or large data gap exists in raw data
- ATMS geolocation error relative to VIIRS is about 3-4km

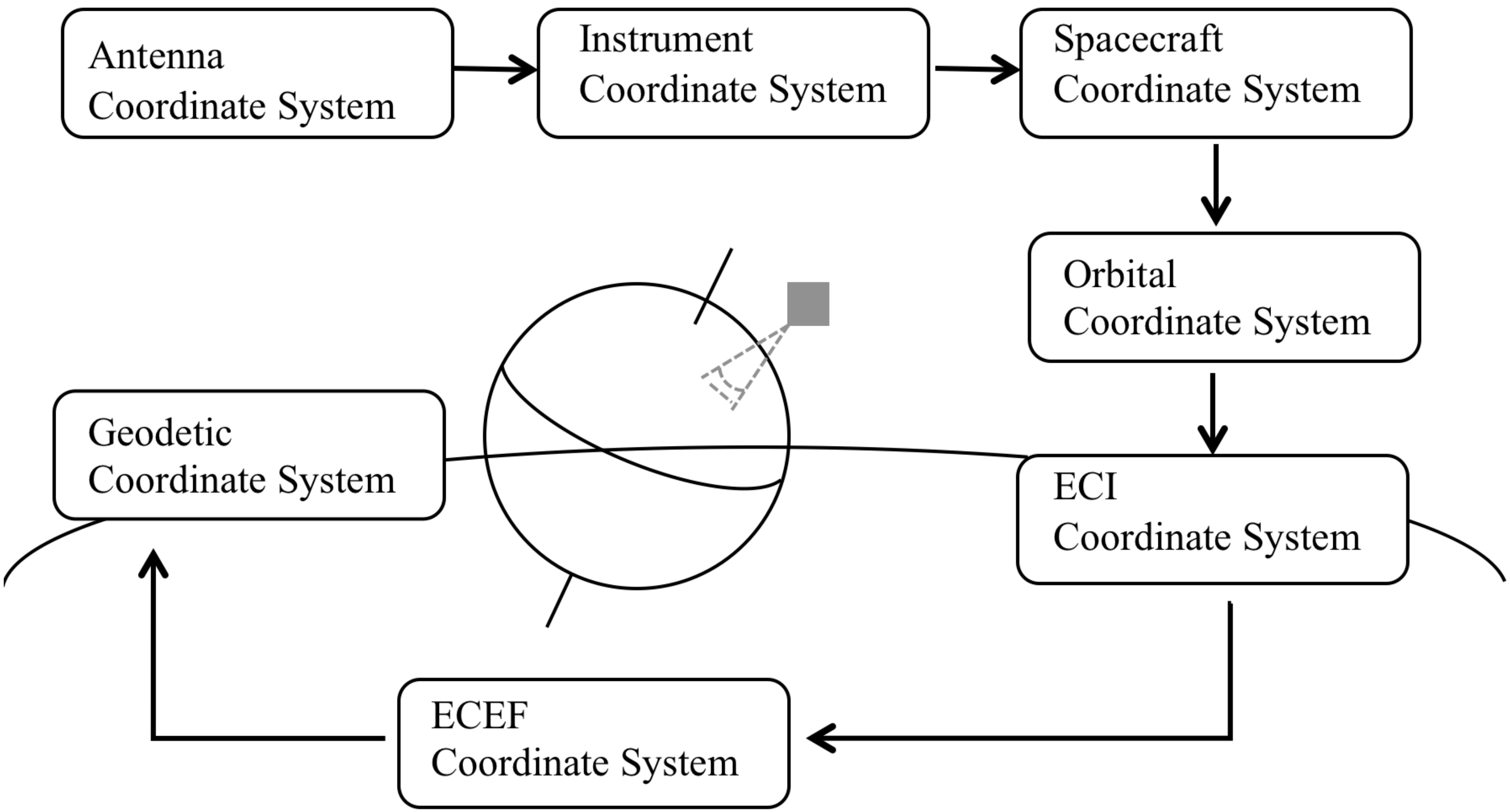

Coordinate Frames Included in Satellite Geolocation

Coordinate system	Schematic plot	Description
Antenna, Instrument and Spacecraft coordinate system	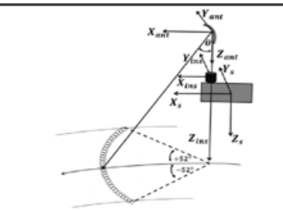	Z_{spc}: space bus down axis X_{spc}: space bus forward axis Y_{spc}: space bus outboard axis Z_{ant}: antenna reflector down axis X_{ant}: same alignment with X_{spc} but perpendicular to Z_{ant} Y_{ant}: cross product of Z_{ant} and X_{ant} Z_{inst}: instrument local down axis X_{inst}: same alignment with X_{spc} but perpendicular to Z_{inst} Y_{inst}: cross product of Z_{inst} and X_{inst}
Orbit coordinate system	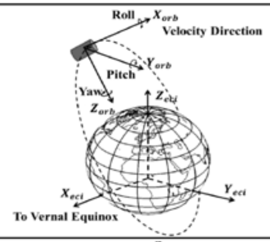	Z_{orb}: from satellite mass center pointing to geodetic center of the Earth X_{orb}: satellite velocity direction Y_{orb}: cross product of Z_{orb} and X_{orb}
Earth Centered Inertial (ECI) coordinate system	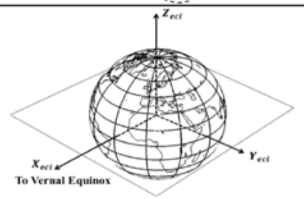	Defined with the Earth's Mean Equator and Equinox at 12:00 Terrestrial time on 1 January 2000 (J2000) X_{ECI}: aligned with the mean equinox Y_{ECI}: rotated by 90° East about the celestial equator Z_{ECI}: aligned with the Earth's spin axis or celestial North Pole
Earth Centered Rotating Coordinate system	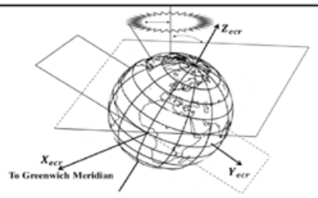	Z_{ECEF}: pointing towards the north X_{ECEF}: intersects the sphere of the Earth at 0° latitude (Equator) and 0° longitude (Greenwich). Y_{ECEF}: Cross product of Z_{ECEF} and X_{ECEF}
Earth ellipsoid and geoid with or without a terrain model coordinate system	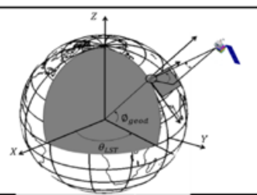	X_{NEZ}: local east Y_{NEZ}: local north Z_{NEZ}: outward from earth center to satellite nadir

Starting with the beam vector at observation time t and position $\hat{p}$ t, $\hat{p}$ in antenna coordinate system

$$\vec{b} = \begin{bmatrix} 0 \\ \sin\theta \\ \cos\theta \end{bmatrix}$$

Based on the established transformation matrixes, the unit vector of instrument viewing beams can be transferred from antenna coordinate system to ECEF coordinate system by applying sequential matrix multiplication:

$$\vec{b}_{ECEF} = T_{ecef/eci} T_{eci/orb} T_{orb/sc} T_{sc/inst} T_{inst/ant} \vec{b}_{ant}$$

Geolocation Accuracy Evaluation- Inflection Point Detection Method

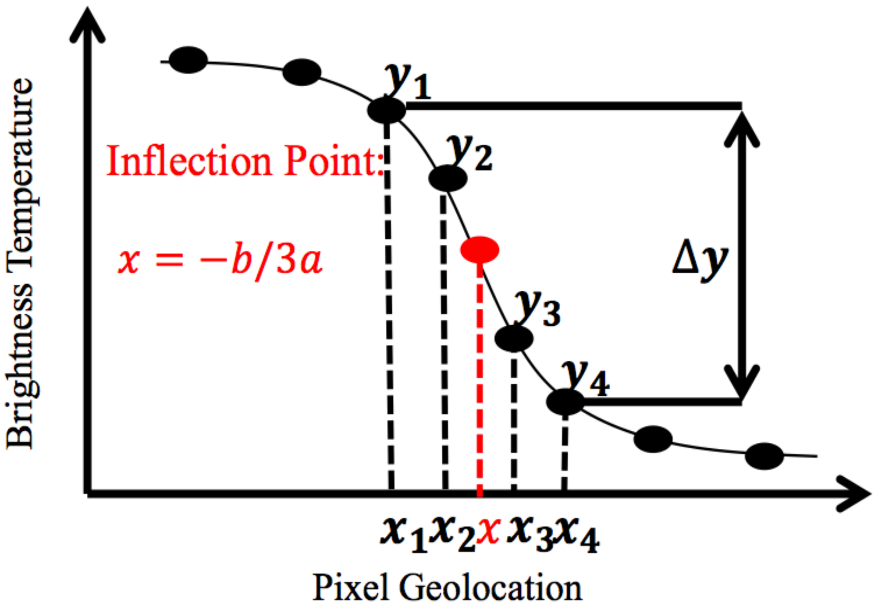

- The coastline signature is modeled using a cubic fit of four consecutive measurement samples along scan line:

$$y_i = ax_i^3 + bx_i^2 + cx_i + d$$
$$(i = 1,2,3,4)$$

y_i is the measurement

x_i is the pixel position (longitude or latitude)

- **The inflection point is considered to be the location of the coastline if :**

$$x = -\frac{b}{3a} \text{ falls } between\ x_2 \text{ and } x_3$$

$\Delta y = |y_1 - y_4|$ exceeds a predefined threshold

- Coefficients are determined:

$$\begin{bmatrix} a \\ b \\ c \\ d \end{bmatrix} = \begin{bmatrix} x_1^3 & x_1^2 & x_1 & 1 \\ x_2^3 & x_2^2 & x_2 & 1 \\ x_3^3 & x_3^2 & x_3 & 1 \\ x_4^3 & x_4^2 & x_4 & 1 \end{bmatrix}^{-1} \begin{bmatrix} y_1 \\ y_2 \\ y_3 \\ y_4 \end{bmatrix}$$

Lawrence H. Hoffman, William L.Weaver and James F. kebler, 1987: Calculation and Accuray of ERBE Scanner Measurement Locations.

Geolocation Accuracy Evaluation- Land-Sea Fraction Method

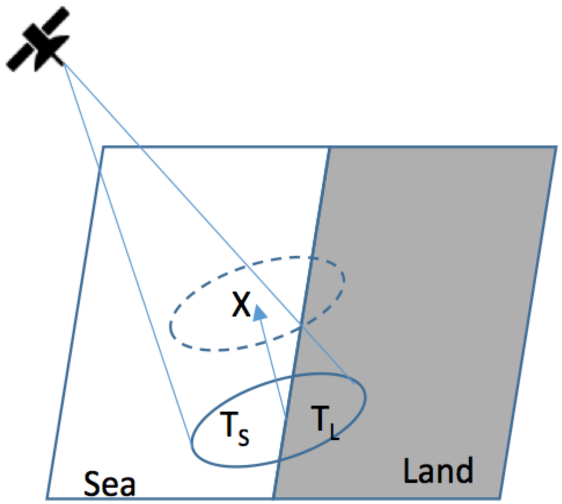

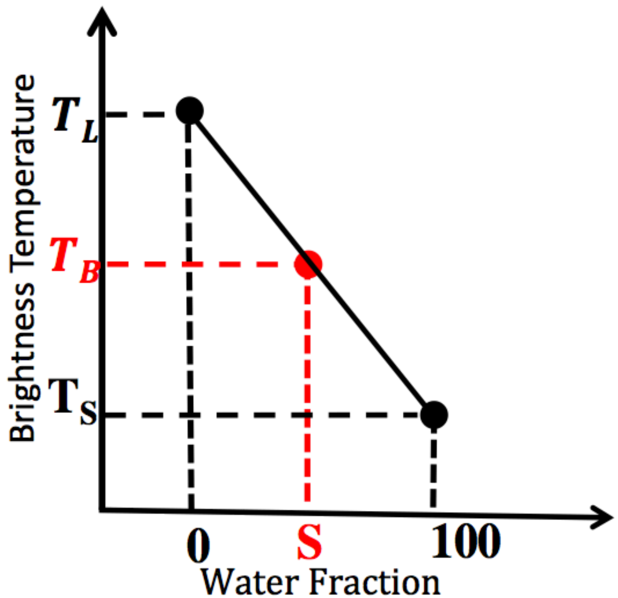

Illustration of the method used to generate synthetic datasets to obtain the navigation uncertainty. Here T_S and T_L are randomly generated using mean values and variances derived from the data and are mixed according to the fraction of water found in the solid footprint. The so-derived synthetic brightness temperature is assigned to the fraction of water calculated from the dashed footprint, which is shifted x km from the solid one in a along-track direction. So T_B may be written as

$$T_B = \frac{S}{100}(T_S - T_L) + T_L$$

RALF BENNARTZ,1999: On the Use of SSM/I Measurements in Coastal Regions

ATMS Geolocation Accuracy

Channel Number	Latitude	Longitude
1	0°	0.01°
2	-0.02°	0.03°
3	0.03°	0.01°
16	0.01°	-0.02°

Full Radiance Calibration

- Calibrated space view scene brightness temperatures from IDPS are not equal to the cosmic background temperature 2.73K
- Abnormal scan angle dependent feature existed in calibrated TDR products

ATMS TDR at Ch18 on February 20, 2012

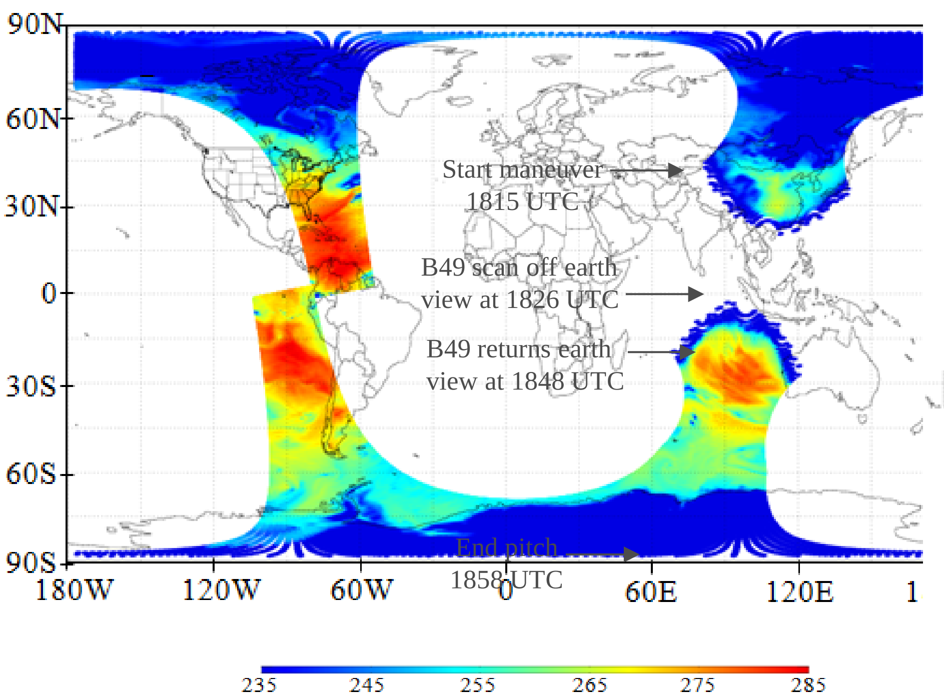

Channel 1

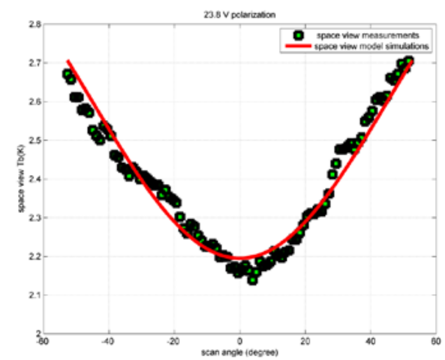

Channel 2

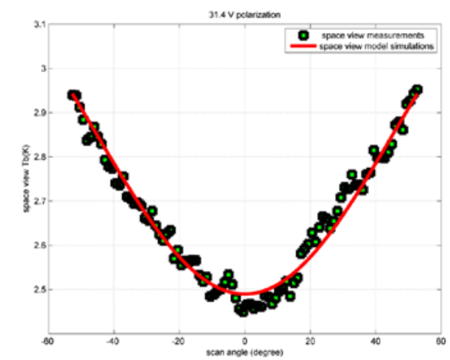

Channel 3

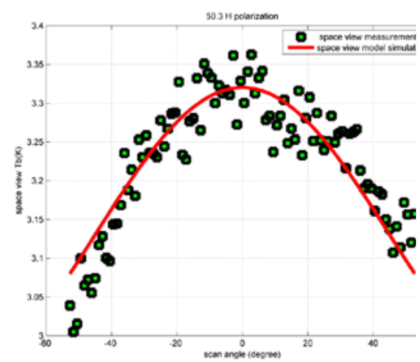

Channel 4

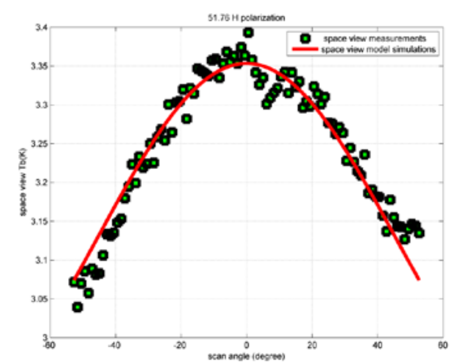

Near Field Radiation Modeling

•An analysis of the ATMS antenna gain measurements reveals that the efficiencies of both ATMS antenna side lobes and cross polarization are frequency-dependent.

•From the ATMS pitch-over maneuver data, it is found that the contributions of spacecraft radiation through the near-field side lobes are significant and dominate the scan angle dependent features in the ATMS antenna temperatures.

•A theoretical model is developed for the conversion from antenna to sensor brightness temperatures, including the angular dependent terms derived from the pitch-over maneuver data.

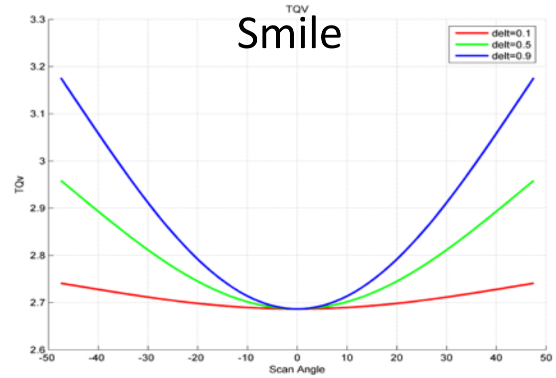

$$\Delta T^{Qv} = \eta_0 + \eta_1 \cdot \sin^2 \theta$$

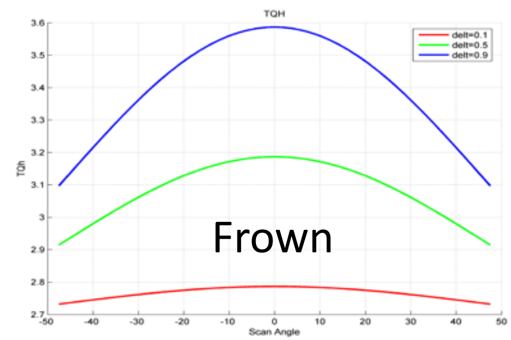

$$\Delta T^{Qh} = \eta_0 + \eta_1 \cdot \cos^2 \theta$$

F. Weng, H. Yang, and X. Zou, 2012, "On convertibility from antenna to sensor brightness temperature for ATMS," IEEE Geosci. Remote Sens. Lett. Vol.10,No.4

From Vince Leslie, Kent Anderson, & Bill Blackwell, June 24, 2013

Flat Reflector Emissivity Model

- ATMS scanning reflector is a gold-plated beryllium flat plate, oriented 45 degrees relative to the wavefront
- Conductive gold surface is a thin layer composed of microcrystalline granules, the emissivity can be expected to significantly exceed the theoretical (Hagen-Rubens) emissivity of a perfectly flat bulk material
- Values of the two polarization components can be expressed in terms of the normal emissivity derived from the Fresnel equations for reflections from a plane interface
- Reflector is scanned relative to a fixed linear polarization feed horn, the resulting Quasi-Vertical (QV) and Quasi-Horizontal (QH) components of emissions are scan angle-dependent (Eq. 1)
- Resulting antenna temperature in Equation 2
  - ε_x is the quasi-V (QV) or quasi-H (QH) emissivity
  - T_{refl} is the physical temperature of the flat reflector

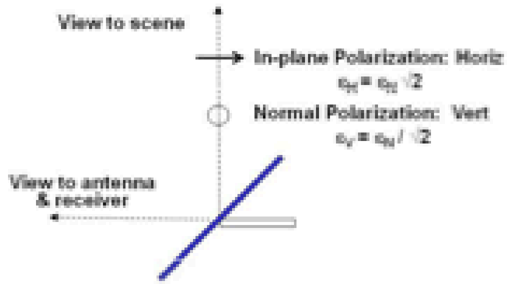

$$\varepsilon_{QV} = \frac{\varepsilon_n}{\sqrt{2}} \times \sin^2(\phi_{scan}) \quad \varepsilon_{QH} = \frac{\varepsilon_n}{\sqrt{2}} \times \cos^2(\phi_{scan}) \quad (1)$$

$$T_{measured} = (1-\varepsilon_x) \times T_{scene} + \varepsilon_x \times T_{refl} \quad (2)$$

Determination of Antenna Emissivity Correction Term From Pitch Maneuver and TVAC Measurements

When scene temperature is close to cold target, the nonlinear term can be ignored and the scene radiance is simply determined from linear two-point calibration equation:

$$R'_{b,I} = R'_c + \frac{R'_w - R'_c}{C_w - C_c}(C_s - C_w)$$

where $R'_{b,I}, R'_w, R'_c$ are corrected scene, warm, and cold target radiance, in which the correction term is modeled as function of emissivity, scan angle and reflector temperature.

For QV

$$R'_{b,I} = R_{b,I} + \varepsilon(f,p)\sin^2\theta_s(R_R - R_{b,I})$$
$$R'_w = R_w + \varepsilon(f,p)\sin^2\theta_w(R_R - R_w)$$
$$R'_c = R_c + \varepsilon(f,p)\sin^2\theta_c(R_R - R_c)$$

For QH

$$R'_{b,I} = R_{b,I} + \varepsilon(f,p)\cos^2\theta_s(R_R - R_{b,I})$$
$$R'_w = R_w + \varepsilon(f,p)\cos^2\theta_w(R_R - R_w)$$
$$R'_c = R_c + \varepsilon(f,p)\cos^2\theta_c(R_R - R_c)$$

where R_R *is reflector thermal radiance,* $\theta_w, \theta_c, \theta_s$ *are* scan angles for warm load, cold target and scene target. In TVAC test, the physical temperature of warm, cold and scene target is measured from PRTs with accuracy of 0.05K, the emissivity then can be determined from equations above.

Antenna Reflector Emissivity Determined From Pitch Maneuver and TVAC Measurements

- Antenna reflector emissivity derived from pitch maneuver and TVAC measurements are consistent with each other;
- Emissivity of QV channels are higher than those of QH channels;
- Emissivity is increase with frequency

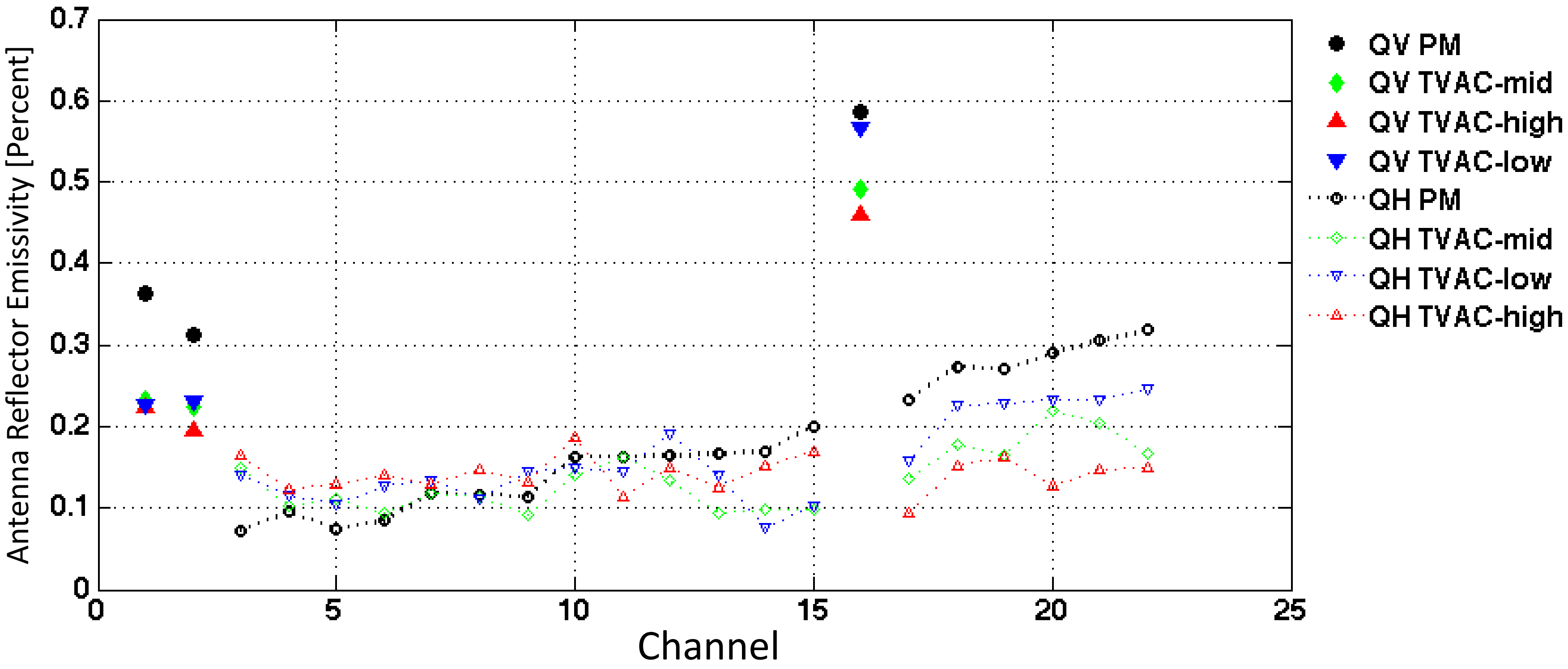

Reflector Emissivity Value

Table.1 Antenna Reflector Emissivity Derived From Pitch Maneuver and TVAC Test Measurements

Channel	Pitch Maneuver	TVAC CP-Mid	TVAC CP-High	TVAC CP-Low
1	0.0036	0.0023	0.0023	0.0023
2	0.0031	0.0022	0.0020	0.0023
3	0.0007	0.0015	0.0014	0.0017
4	0.0010	0.0010	0.0012	0.0012
5	0.0007	0.0011	0.0011	0.0013
6	0.0008	0.0009	0.0013	0.0014
7	0.0012	0.0012	0.0013	0.0013
8	0.0012	0.0011	0.0011	0.0015
9	0.0011	0.0009	0.0015	0.0013
10	0.0016	0.0014	0.0015	0.0019
11	0.0016	0.0016	0.0014	0.0011
12	0.0016	0.0013	0.0019	0.0015
13	0.0017	0.0009	0.0014	0.0012
14	0.0017	0.0010	0.0008	0.0015
15	0.0020	0.0010	0.0010	0.0017
16	0.0059	0.0049	0.0046	0.0057
17	0.0023	0.0014	0.0016	0.0009
18	0.0027	0.0018	0.0023	0.0015
19	0.0027	0.0016	0.0023	0.0016
20	0.0029	0.0022	0.0023	0.0013
21	0.0031	0.0020	0.0023	0.0015
22	0.0032	0.0017	0.0025	0.0015

New Two-Point Calibration Model in ARTS

Antenna emission is modeled as function of scan angle and reflector temperature. Cold space observations from pitch maneuver operation are used to derive model parameters for different channels

Revised Two Point Calibration Equation in ARTS

For Vertical Polarization Channels:

$$R_s = \frac{1}{1-\varepsilon_f \sin^2\theta_s}\left[\delta\left(R'_h - R'_c\right) + R'_c - \varepsilon_f \sin^2\theta_s\right]$$

For Horizontal Polarization Channels:

$$R_s = \frac{1}{1-\varepsilon_f \cos^2\theta_s}\left[\delta\left(R'_h - R'_c\right) + R'_c - \varepsilon_f \cos^2\theta_s\right]$$

Rs: Calibrated antenna radiance

R'_h: Corrected Warm load radiance,

R'_c: Corrected Cold space radiance

$$R'_g = R_g + \begin{cases} \varepsilon_f \sin^2\theta_g\left(R_{rfl} - R_g\right), & QV\ pol \\ \varepsilon_f \cos^2\theta_g\left(R_{rfl} - R_g\right), & QH\ pol \end{cases}, \text{g=h,c}$$

θ_h: Scan angles of warm load measurements

θ_c: Scan angles of space view

θ_s: Scan angles of Earth view (i.e., each FOV)

δ: Defined as (Cs - Cc) /(Ch - Cc), where Ch/Cc/Cs are receiver output counts of warm load, cold space and earth view, respectively

Space View BT Calibrated by ARTS

Channel -1

ARTS IDPS

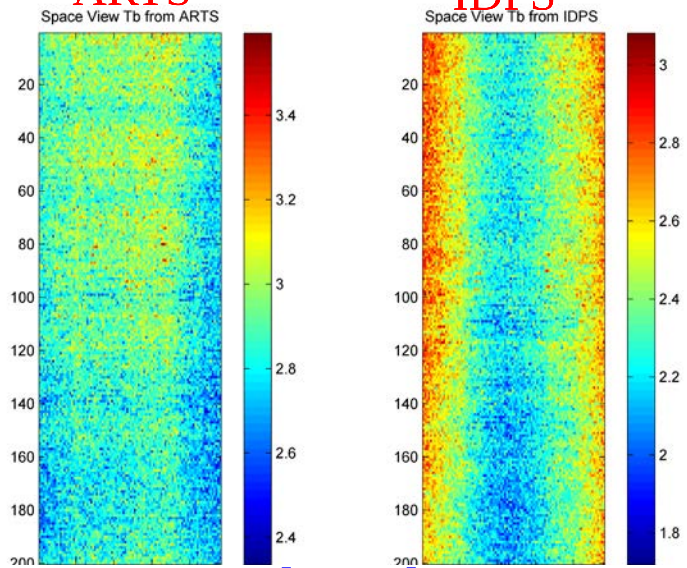

Channel -2

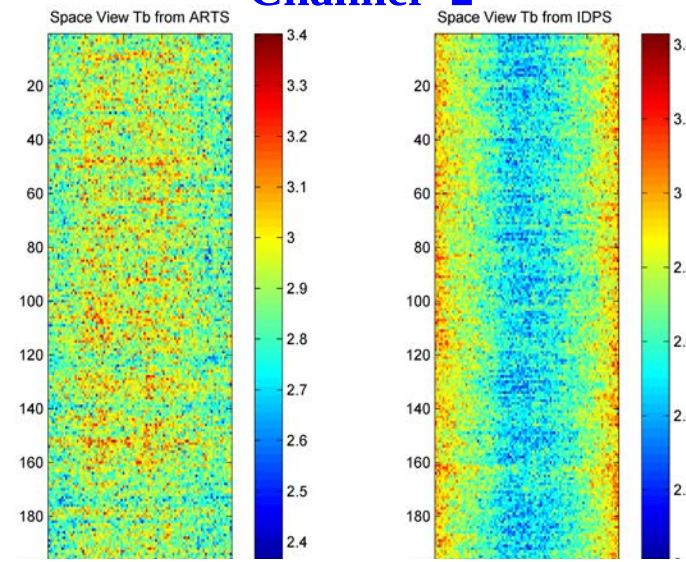

Channel -14

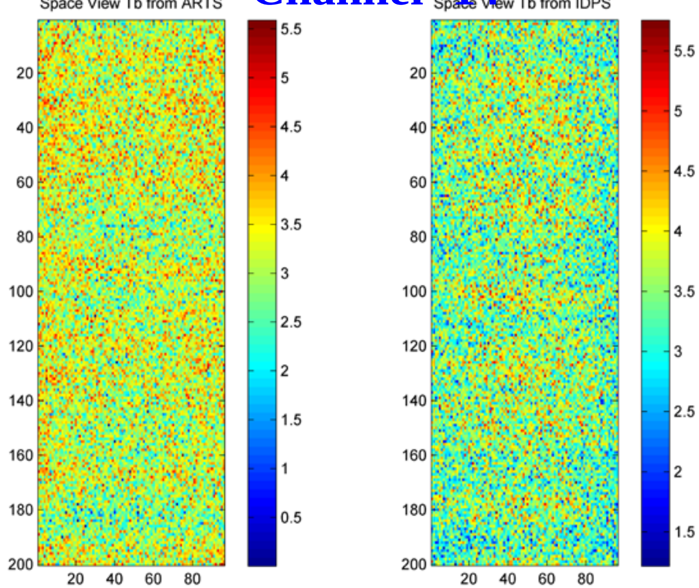

Channel -18

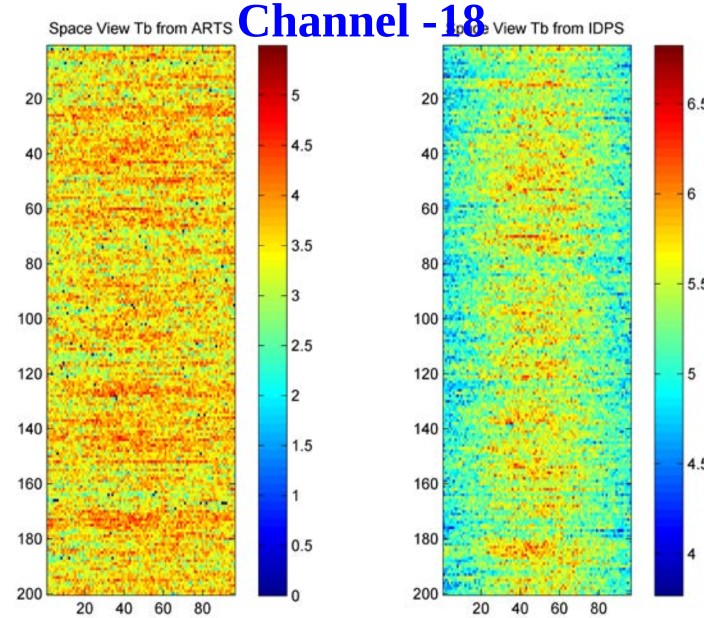

Scan Angle Dependent in TDR from ARTS

For space view BT corrected by ARTS: No scan angle dependent feature, and close to cosmic background 2.73K

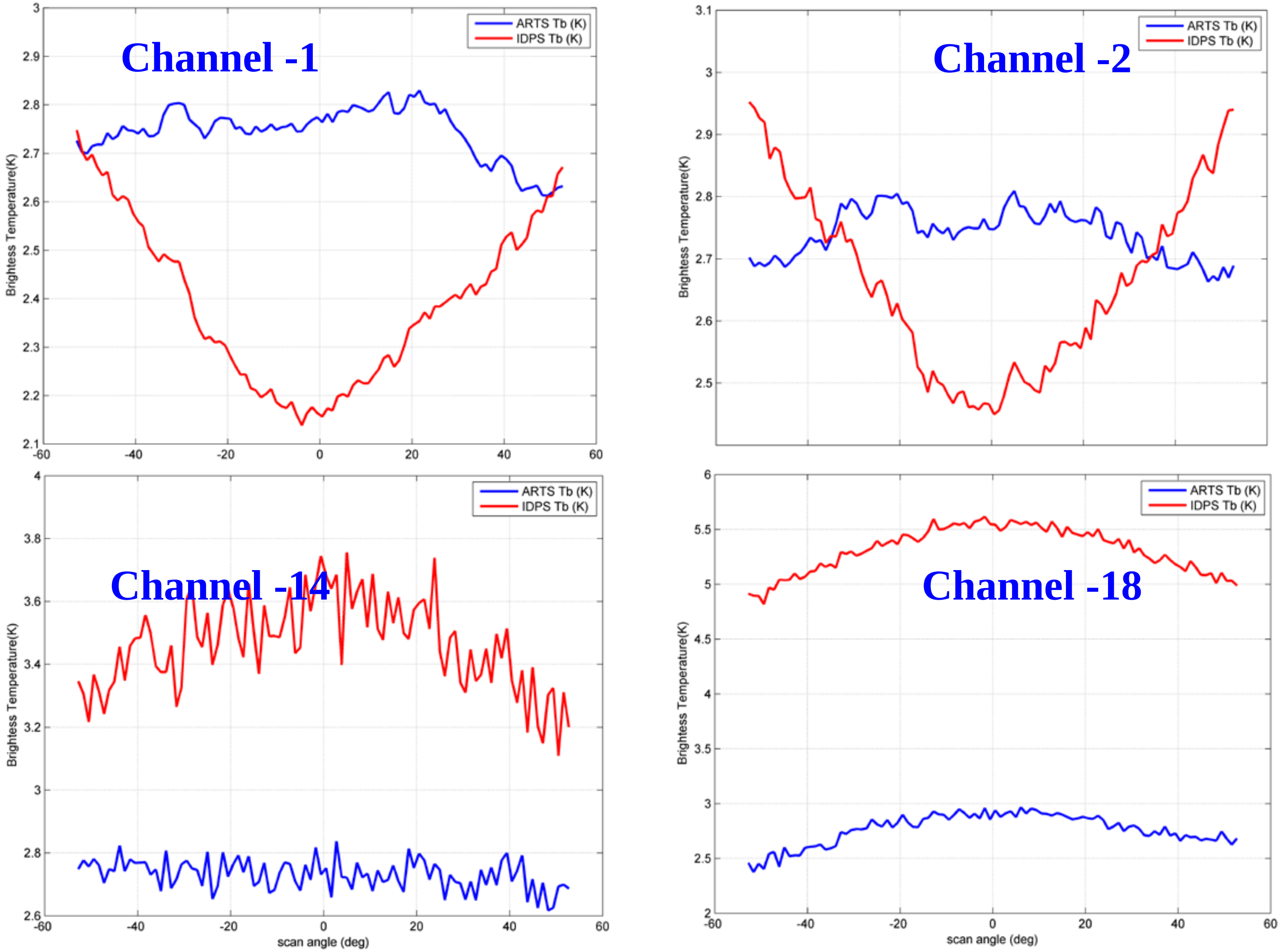

Determination of Nonlinearity Correction Parameters

- Taken PRT measurements of scene temperature T_s as truth, nonlinearity at 11 different scene temperature are computed as $Qb = Ts - T_{b,l}$
- For Q_b computed without antenna radiation correction, nonlinearity errors in cold end are not converged to zero, indicate the possible contamination of receiver output counts
- Correction of antenna radiation term can reduce the nonlinearity error in a certain degree, especially for measurements at cold end. Correction quantity is depend on temperature difference between reflector and scene target

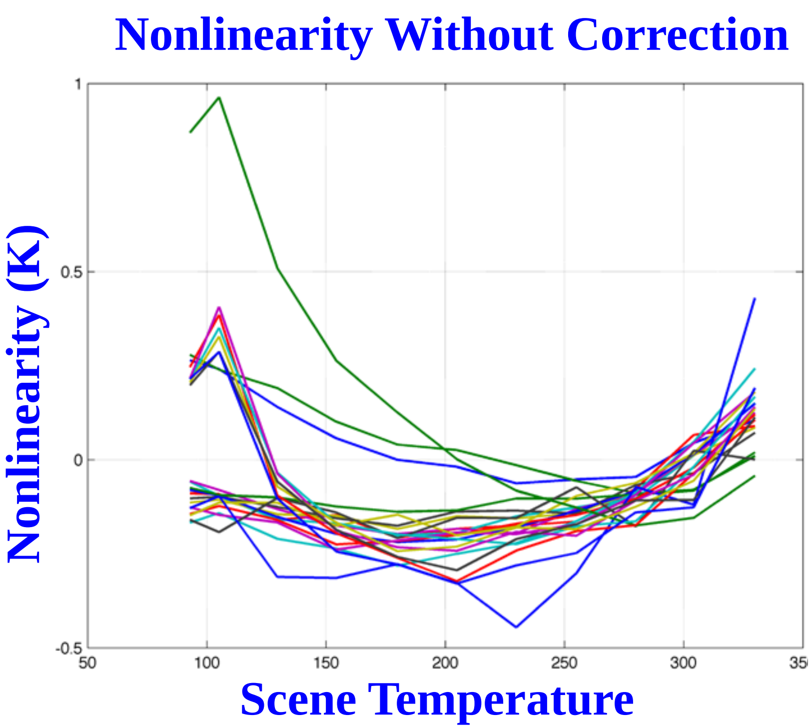

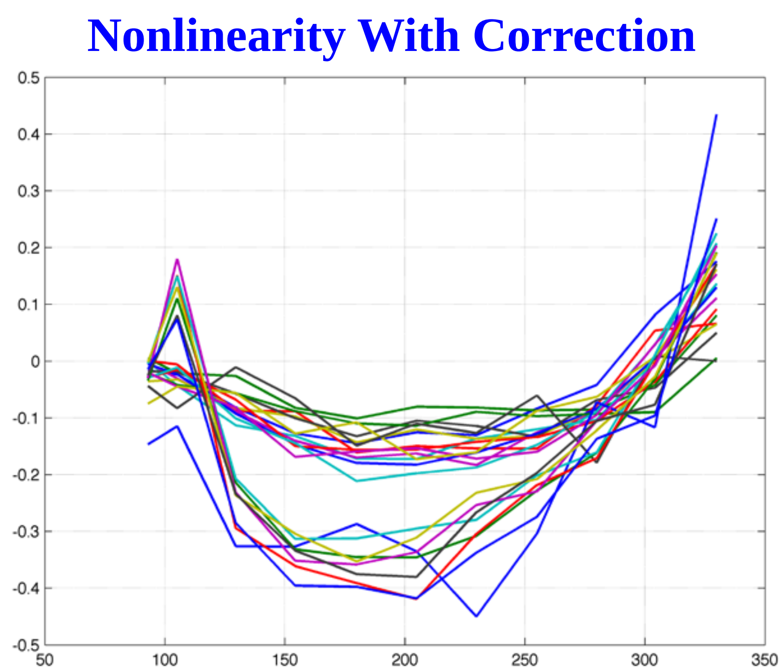

μ Parameter Based Nonlinearity Correction Equations

The two-point calibration is derived in brightness temperature form as

$$R_b = R_w + G_b^{-1}(C_s - C_w) + Q_b = R_{b,I} + Q_b$$

where the linear and nonlinear terms are expressed as

$$R_{b,I} = R_w + G_b^{-1}(C_s - C_w)$$

$$G_b = \frac{C_w - C_c}{R_w - R_c} \qquad x = \frac{R_{b,I} - R_c}{R_w - R_c}$$

The maximum nonlinearity value can be derived by performing the derivative with respect to x.

Using Taylor's expansion for f(x) = x(x-1) at x_0=0.5

$$Q_b = \mu G_b^{-2}(C_s - C_w)(C_s - C_c) = \mu(R_w - R_c)^2 x(x-1)$$

$$Q_b = Q^{\max}[4 \cdot (x-0.5)^2 - 1]$$

$$Q^{\max} = \frac{1}{4} \cdot \mu \cdot (R_w - R_c)^2$$

F. Weng et al. "Calibration of Suomi national polar-orbiting partnership advanced technology microwave sounder." Journal of Geophysical Research: Atmospheres 118.19 (2013): 11-187.

Prediction of μ from Receiver Temperature

- "μ" is a function of instrument temperature $\mu = a_2 T^2 + a_1 T + a_0$ (Unit of T is ^{o}C)

Channel	a2	a1	a0
1	9.51E-09	4.68E-08	1.50E-05
2	3.36E-08	4.46E-07	-6.15E-07
3	-4.64E-09	3.99E-07	9.05E-06
4	4.93E-09	5.09E-08	1.37E-05
5	-6.64E-11	1.94E-07	1.35E-05
6	-2.23E-09	2.64E-07	7.61E-06
7	4.71E-09	2.88E-08	7.02E-06
8	2.63E-09	6.90E-08	1.39E-05
9	5.07E-09	9.45E-09	3.46E-06
10	1.07E-08	1.96E-08	1.03E-05
11	4.87E-09	-1.97E-09	1.65E-05
12	8.30E-09	-1.43E-08	1.30E-05
13	-9.06E-09	4.45E-07	9.81E-06
14	-1.20E-08	1.88E-08	1.35E-05
15	-2.10E-08	4.71E-07	3.04E-05
16	-1.80E-08	1.01E-06	2.30E-05
17	-1.78E-08	9.82E-07	2.38E-05
18	-3.60E-08	1.29E-06	2.19E-05
19	-4.24E-08	1.43E-06	2.43E-05
20	-3.15E-08	1.22E-06	2.42E-05
21	-2.40E-08	1.00E-06	2.34E-05
22	-4.37E-08	1.23E-06	2.80E-05

Predicted On-orbit ATMS Nonlinearity

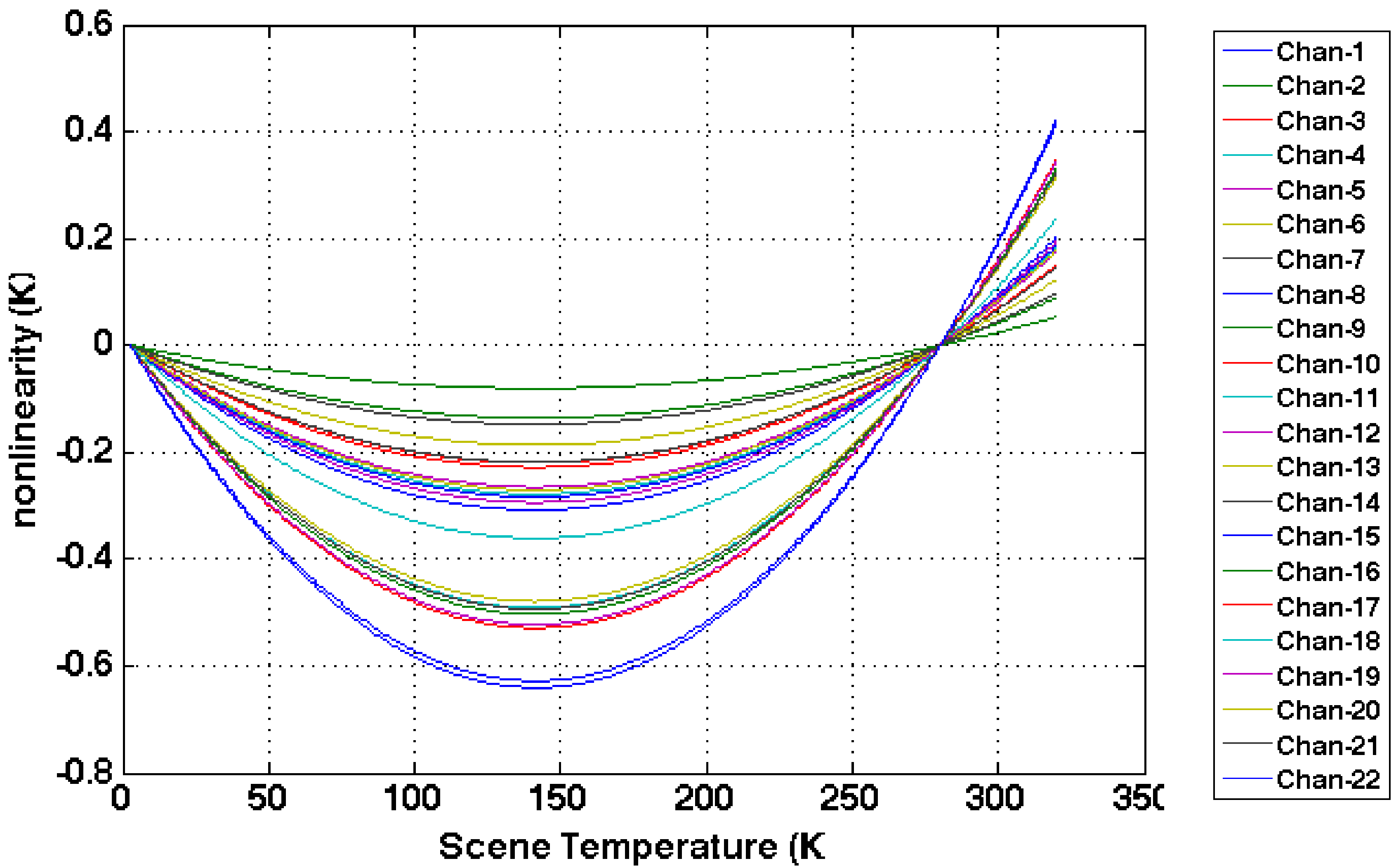

Maximum Nonlinearity

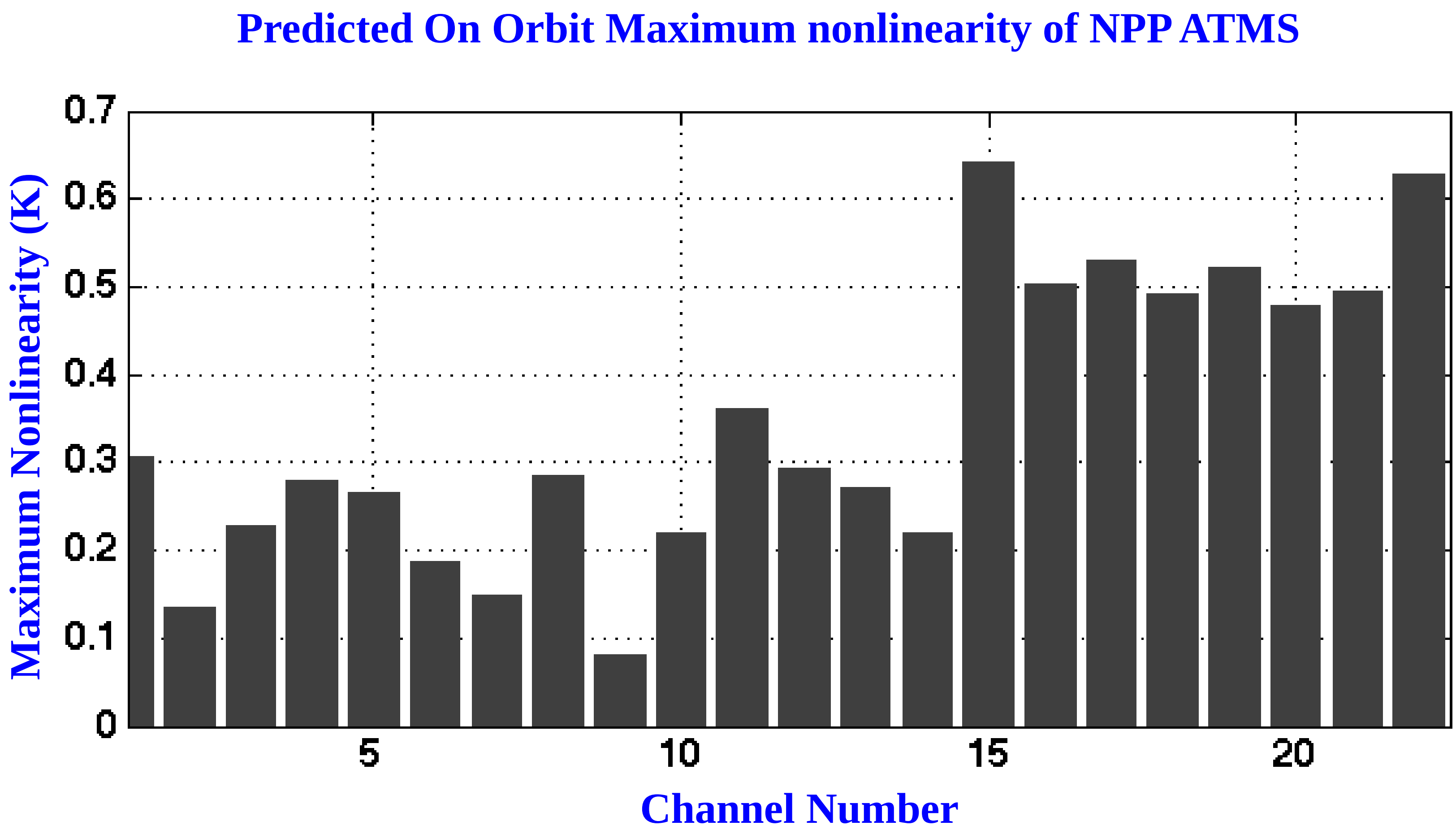

TDR Remapping

Resolution Reduction

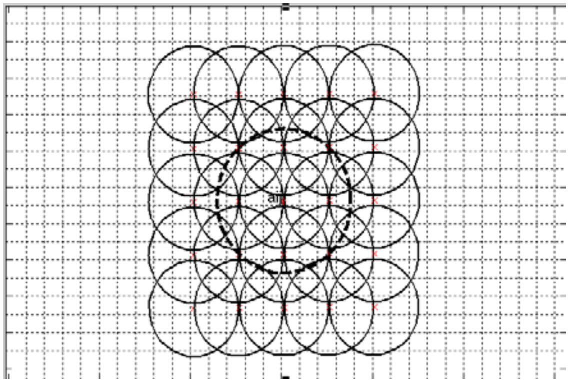

FOV 2.2°

Resolution Enhancement

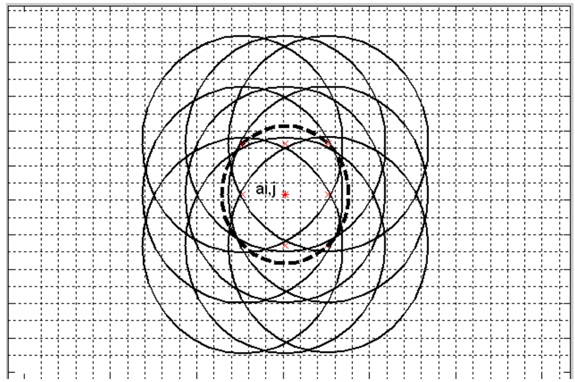

FOV 2.2°

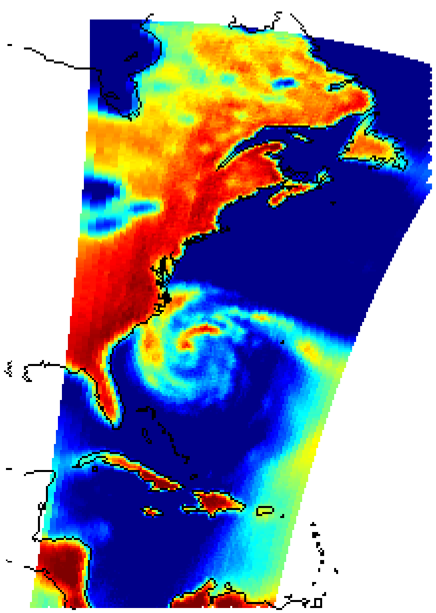

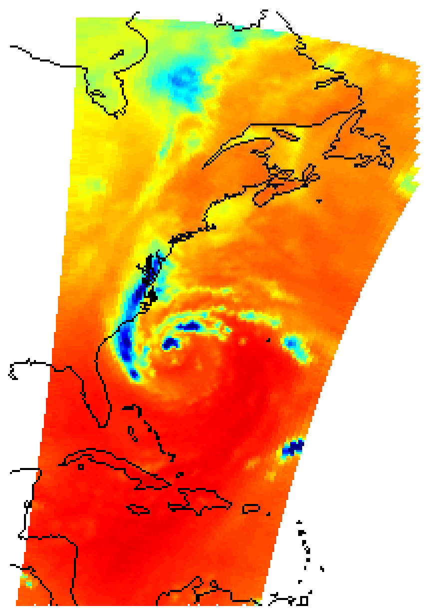

- Explore the potential of the oversampling characteristic of ATMS observations and generate observations at different frequencies with consistent FOV size
- Backus-Gilbert observation reconstruction algorithm is used for remapping TDR to expected spatial resolution
- Remapping coefficients are tuned to ensure the remapped TDR products are in best balance between noise and spatial resolution

Hu Yang and Xiaolei Zou, “OPTIMAL ATMS REMAPPING ALGORITHM FOR CLIMATE RESEARCH”, IEEE TRANSACTIONS ON GEOSCIENCE AND REMOTE SENSING, VOL. 52, NO. 11, NOVEMBER 2014

Coherent Noise Filtering

Based on frequency spectrum analysis of the receiver output calibration counts, a low-pass filter with sinc window function is developed to effectively remove the high-frequency components (rapid fluctuations) while keep the low-frequency components (gain variations) unchanged.

Sinc Window Function

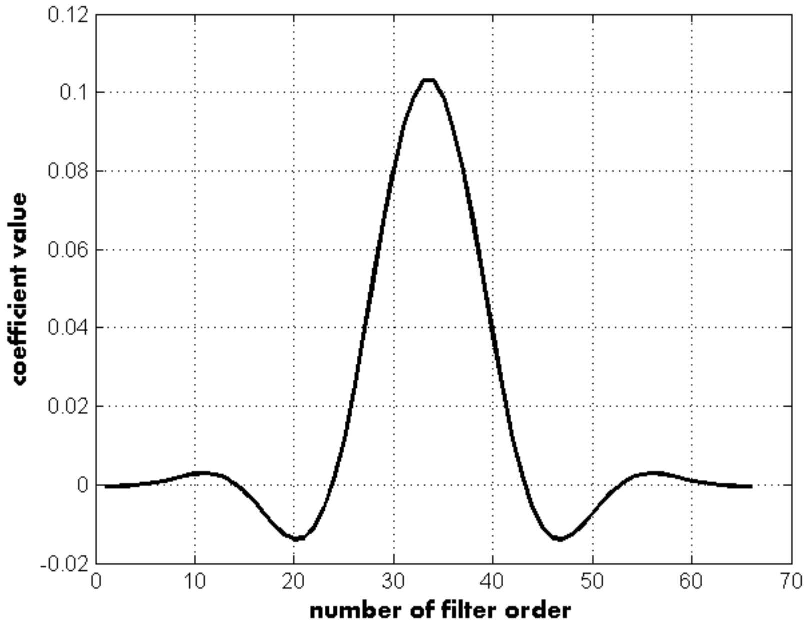

Calibrated Tb with and without calibration counts noise filtering

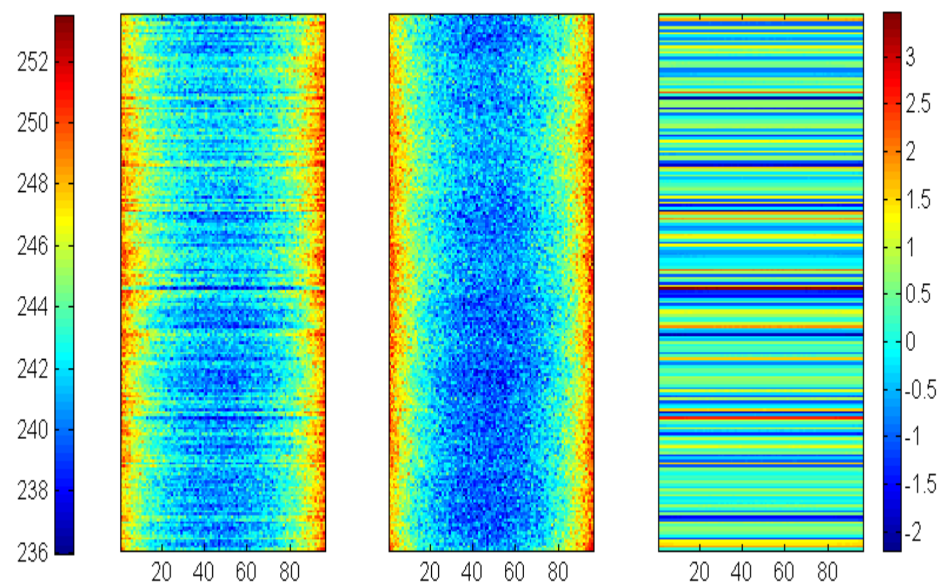

Lunar Contamination Correction

Brightness temperature increment arising from lunar contamination is modeled as function of lunar solid angle, antenna response and radiation from the Moon

$$\Delta T_{moon} = G * \Omega * T_{moon}$$

G: Antenna response function

Ω_{moon} Weights of the Moon in antenna pattern:

T_{moon}: Brightness temperature of the Moon

- LI happens when $\beta = \beta - \alpha_{lc} \leq 1.25 \cdot \theta_{3dB}$
- Lunar contamination impacts to the four space view counts are different.
- The increased brightness temperature due to the lunar contamination can be accurately identified and quantified from the model.

Sketch plot of lunar contamination in space view

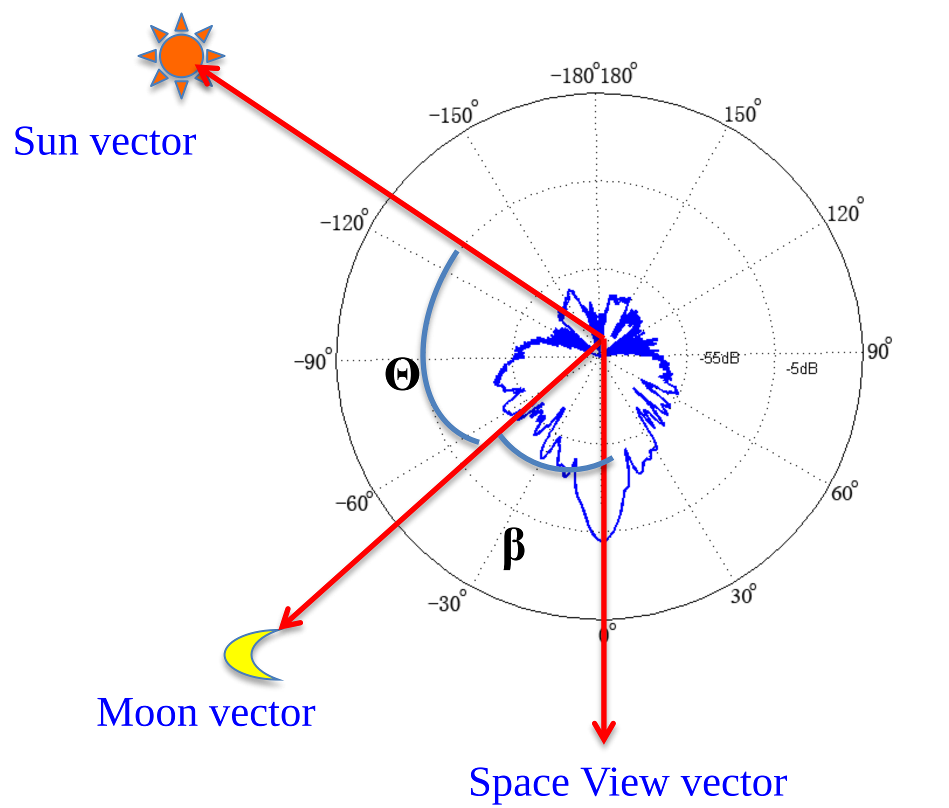

Hu Yang and Fuzhong Weng, 2014, “On-Orbit ATMS Lunar Contamination Corrections”, Submitted to IEEE Transaction on Geoscience and Remote Sensing

ATMS SDR Lunar Intrusion Identification and Correction Activities and Results

Activities

- ATMS RDR dataset was re-processed using the latest ATMS SDR algorithm code and PCT to evaluate lunar intrusion (LI) detection and correction performance
- The potential impact of current TDR with LI on NWP model was evaluated in GSI
- New metrics and physical model was developed for LI identification and correction
- Different approaches for LI correction was compared and tested in ARTS, optimal algorithm was selected and implemented in current operational calibration system

Results

- Lunar intrusion was accurately identified and correctly flagged in SDR datasets
- Data gap was removed after LI correction, residual correction error is below the instrument noise
- New scheme for LI detection and correction was developed for future improvement of current IDPS

ICVS Monitoring Results of Lunar Intrusion

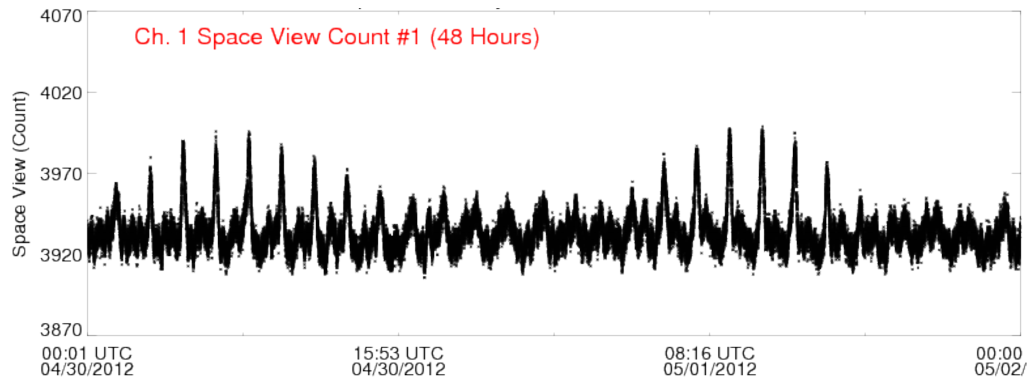

Operational SDR without LI correction

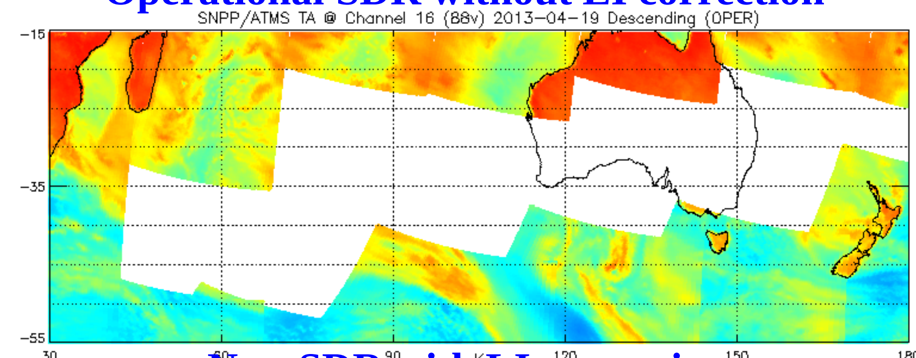

New SDR with LI correction

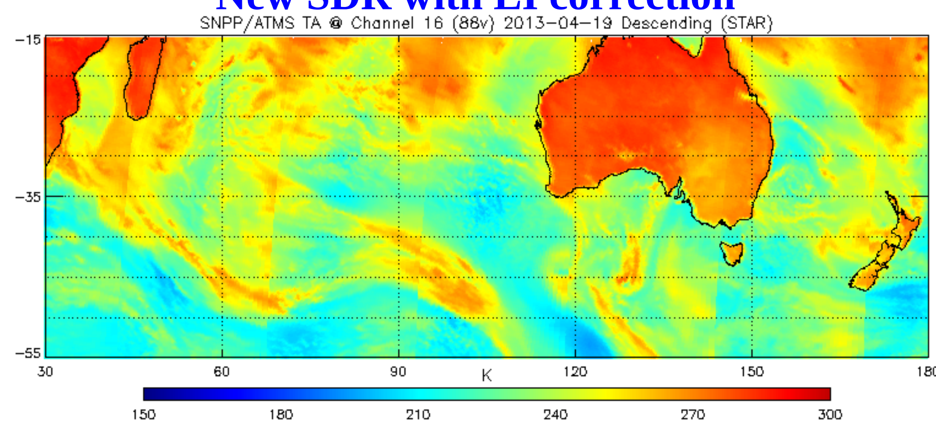

Conclusions and Future Works

- ARTS is a full radiance calibration system designed for microwave sounding instruments. With new sciences developed from solid study of SNPP ATMS, the calibration accuracy of TDR products from future JPSS satellite will be improved

- ARTS is designed as a robust, sustainable and scientifically defensible operational calibration system for future JPSS satellite, and also can be used as test bed for developing new algorithm.

- Future work will focus on reprocessing SNPP ATMS data using ARTS, generating 2.2^{o} resolution TDR products for use in weather and climate study

Pertinent Publications

- Fuzhong Weng, Hu Yang, Xiaolei Zou, 2012, "On Convertibility From Antenna to Sensor Brightness Temperature for ATMS", IEEE Geoscience and Remote sensing Letters, Vol.99, pp 1-5

- Fuzhong Weng, Xiaolei Zou, Ninghai Sun, Hu Yang, Xiang Wang, Lin Lin, Miao Tian, and Kent Anderson, 2013, "Calibration of Suomi National Polar-Orbiting Partnership (NPP) Advanced Technology Microwave Sounder (ATMS) ", Journal of Geophysical Research, Vol.118, No.19, PP. 11,187~11,200

- Fuzhong Weng, Xiaolei Zou, 2013, "Errors from Rayleigh-Jeans approximation in satellite microwave radiometer calibration systems", 52 (3) PP. 505-508

- Hu Yang and Xiaolei Zou, 2014, "OPTIMAL ATMS REMAPPING ALGORITHM FOR CLIMATE RESEARCH", IEEE Transaction on Geoscience and Remote sensing

- Xiaolei Zou, Fuzhong Weng, and Hu Yang, 2014, "Connection the Time Series of Microwave Sounding Observations from AMSU to ATMS for Long-Term Monitoring of Climate Change", Journal of Climate, accepted for publication

- Hu Yang and Fuzhong Weng, 2014, "On-Orbit ATMS Lunar Contamination Corrections", Submitted to IEEE Transaction on Geoscience and Remote Sensing